NATIONAL ADVISORY COMMITTEE FOR AERONAUTICS

TECHNICAL NOTE 4385

COMPARISON OF SHOCK-EXPANSION THEORY WITH EXPERIMENT FOR THE LIFT, DRAG, AND PITCHING-MOMENT CHARACTERISTICS OF TWO WING-BODY COMBINATIONS AT M = 5.0

By Raymond C. Savin

Ames Aeronautical Laboratory
Moffett Field, California

Washington

September 1958

NATIONAL ADVISORY COMMITTEE FOR AERONAUTICS

TECHNICAL NOTE 4385

COMPARISON OF SHOCK-EXPANSION THEORY WITH EXPERIMENT FOR THE LIFT, DRAG, AND PITCHING-MOMENT CHARACTERISTICS OF TWO WING-BODY COMBINATIONS AT M = 5.0

By Raymond C. Savin

SUMMARY

Lift, drag, and pitching-moment coefficients for two wing-body combinations were determined from tests at a Mach number of 5.0 and angles of attack up to 9°. The test models consisted of small thin wings mounted on a body composed of a fineness-ratio-3 ogival nose and a fineness-ratio-2 cylindrical afterbody. The wings were symmetrically mounted on the cylindrical portion of the body and had triangular and trapezoidal plan forms.

The results of these tests are compared with results obtained by a relatively simple application of the generalized shock-expansion method in combination with the T' method of evaluating the skin-friction drag coefficients. Good agreement between theory and experiment is obtained for the total drag coefficients over the test angle-of-attack range. Theory and experiment are also found to be in good agreement for the lift and pitching-moment coefficients at the lower angles of attack. At the higher angles of attack, the theoretically determined coefficients are somewhat higher than those obtained experimentally.

INTRODUCTION

The generalized shock-expansion method has proven to be a useful tool in the calculation of flow about airfoils and bodies of revolution at high supersonic Mach numbers (see, e.g., refs. 1 and 2). Experimental lift, drag, and pitching-moment coefficients for two wing-body combinations were obtained in the Ames 10- by 14-inch supersonic wind tunnel at a Mach number of 5.0 and angles of attack up to 9°. The models consisted of small triangular and trapezoidal plan-form wings mounted on an ogive-cylinder. Both wings were entirely immersed in the flow field generated by the body. A comparison of the results of these tests with those obtained by means of the generalized shock-expansion method is the subject of the present paper.

NOTATION

C_D drag coefficient, $\frac{\text{drag}}{q_\infty \pi (d^2/4)}$

C_L lift coefficient, $\frac{\text{lift}}{q_\infty \pi (d^2/4)}$

C_m pitching-moment coefficient, $\frac{\text{moment about vertex}}{q_\infty \pi (d^2/4) l}$

d maximum diameter of body, in.

l maximum length of body, in.

M Mach number (ratio of local velocity to local speed of sound)

p_t total pressure, lb/sq in.

q dynamic pressure, lb/sq in.

V local resultant velocity, ft/sec

w velocity component normal to plane of wings at the vertex, positive upward, ft/sec

α angle of attack, radians unless otherwise specified

δ_N semivertex angle of body

ϵ upwash angle, radians unless otherwise specified

σ sidewash angle (i.e., angle of flow inclination in plane of wings measured with respect to body axis), radians unless otherwise specified

Subscripts

∞ free-stream conditions

f due to skin-friction forces

P due to pressure forces

S conditions immediately downstream of the shock wave

APPARATUS AND TESTS

The tests were conducted in the Ames 10- by 14-inch supersonic wind tunnel. A detailed description of the wind tunnel and auxiliary equipment may be found in reference 3. Aerodynamic forces and moments acting on the models were measured by means of a three-component strain-gage balance.

The test models, shown in figure 1, were constructed of steel and were composed of thin, simple wedge-shaped wings mounted on a body consisting of a fineness-ratio-3 circular-arc ogival nose and a fineness-ratio-2 cylindrical afterbody. The wings had triangular and trapezoidal plan forms and were symmetrically mounted on the body. The root sections were 3 percent thick in streamwise planes and were equal in length to the cylindrical portion of the body. The leading edges of the wings were of constant thickness equal to 0.004 inch.

Lift, drag, and pitching-moment coefficients were determined for both models at a Mach number of 5.0 and at angles of attack to 9°. The free-stream Reynolds number based on the length of the body was 1.6 million. Axial forces acting on the body base, as determined by the difference between measured base pressures and free-stream static pressures, were subtracted from measured total forces. The data presented, therefore, do not include body-base drag.

The variation in Mach number from the nominal value did not exceed ±0.03 in the region of the test section where the models were located. The deviation in free-stream Reynolds number did not exceed ±30,000. Errors in angle of attack due to uncertainties in corrections for stream angle and for deflection of the model support system were less than ±0.2°.

The precision of the experimental force and moment coefficients was affected by inaccuracies in the force measurements obtained with the balance system, as well as uncertainties in the determination of free-stream dynamic pressures and base pressures. The resulting maximum errors were estimated to be ±0.02 for all three coefficients, C_L, C_D, and C_m. In general, the experimental results presented herein are in error by less than these estimates.

APPLICATION OF THE GENERALIZED SHOCK-EXPANSION METHOD

It was demonstrated in reference 2 that the generalized shock-expansion method is applicable to bodies of revolution provided that the similarity parameter $M_\infty \delta_N$ is about 1 or greater. It was also shown that streamlines can be approximated by meridian lines provided that the angle of attack is small. For the present configurations, the influence of the wings on the body is considered small and, therefore, neglected. Thus, flow conditions on the body, as well as conditions in the plane of

the wings, were calculated in the manner discussed in reference 2 for a free-stream Mach number of 5.0.

The results of the calculations of the flow about the body in the plane of the wings are shown in figures 2 and 3 for angles of attack of 5° and 10°. Figure 2 shows the orientation of the wings with respect to the shock waves generated by the body. The distributions of the sidewash angle, Mach number, and total pressure ratio along the respective wing leading edges are shown in figure 3. It is clear from figure 3 that the sidewash angle, σ, is always less than 6°. Thus, the velocity at any spanwise station associated with the Mach number at that station may be taken parallel to the body axis with but little loss in accuracy for purposes of calculating pressures. It will be noted in figure 3(c) that the gradient of the total-pressure ratio is infinite at the surface of the body. This can be demonstrated from considerations of continuity and configuration geometry. There remains only the determination of the upwash angle in order to calculate the pressure coefficients and, hence, the forces acting on the wings. Now in the application of the shock-expansion method along meridian lines on bodies of revolution, only the magnitude of the resultant velocity is considered to change along the body (see ref. 2). Thus, the upwash angle is considered constant along the body and its value is that at the vertex. In the present application, then, the upwash angle at the leading edge of the root chord (wing-body juncture) was calculated from the conical flow solution at the vertex (see, e.g., ref. 4), and may be expressed in the form

$$\epsilon \cong \frac{w}{V}$$

where w is the crossflow component of velocity at the vertex in the side meridian plane (i.e., in the plane of the wings), and V is the resultant velocity at this point. The upwash angle at the tips of the wings can be calculated for the cases considered here since the tips lie, for all practical purposes, immediately behind the shock wave (see fig. 2). Thus, in this region

$$\epsilon \cong \frac{V_\infty \alpha}{V_s}$$

where M_s and, hence, V_s are known from the solution of the flow generated by the body (see fig. 3). The local upwash angle can then be determined if the spanwise variation is assumed to be the Beskin type (see, e.g., ref. 5). In other words, the upwash angle is assumed to vary inversely as the square of the spanwise distance. This variation is shown plotted in figure 4 for both wings at $\alpha = 5^\circ$ and $\alpha = 10^\circ$. With flow conditions at the leading edges thus established, the pressure coefficients on the windward and leeward sides of the wings can be calculated at each spanwise station. In the present cases, the streamlines on the wings have essentially the direction of the free stream (see ref. 2). The pressure coefficients downstream of the leading edge are therefore considered

constant at each spanwise station, but vary with spanwise distance since the Mach number and total pressure vary along the leading edge (see fig. 3).

The lift, pressure drag, and pitching-moment coefficients have been determined by the integration of the pressure coefficients over the body and on the wings. Skin-friction drag coefficients were calculated by the T' method of Rubesin and Johnson (ref. 6), as modified by Sommer and Short (ref. 7), with the assumption that laminar flow prevailed over the entire body and turbulent flow existed over the wings. This assumption is somewhat arbitrary. It should be mentioned, however, that recent visual flow studies on a comparable configuration under similar conditions indicated that the flow was essentially of the type assumed for the present configurations. The skin-friction drag coefficient was evaluated at $\alpha = 0^\circ$ and was assumed to be independent of angle of attack. The results of the foregoing calculations showing the contribution to the total forces of the body and the wings are shown in the following table.

	Body				Triangular Wings				Trapezoidal Wings			
α, deg	C_L	C_{D_P}	C_{D_f}	C_m	C_L	C_{D_P}	C_{D_f}	C_m	C_L	C_{D_P}	C_{D_f}	C_m
0	0	0.082	0.015	0	0	0.003	0.025	0	0	0.002	0.026	0
5	.252	.115	.015	-.135	.210	.021	.025	-.184	.230	.022	.026	-.186
10	.546	.202	.015	-.284	.431	.079	.025	-.381	.476	.086	.026	-.386

The leading-edge drag and drag due to wing thickness are small and were neglected in the calculations. Thus, C_{D_P} presented in the table for the wings at $\alpha = 0^\circ$ represents only the base drag which was evaluated on the assumption that the base-pressure coefficient is equal to 70 percent of the vacuum-pressure coefficient. The body-base drag was omitted throughout. All the coefficients presented in the table are referred to body-base area.

DISCUSSION

The calculated and experimentally determined lift, drag, and pitching-moment coefficients for the complete configurations at a Mach number of 5.0 are presented in figure 5. The generalized shock-expansion method, employed in combination with the T' method of evaluating the skin-friction drag coefficient, yields good agreement with experimental results for the total-drag coefficient over the test angle-of-attack range. It should be noted that the results presented in reference 2 that the shock-expansion method yields results which are in good agreement with experiment for the pressure drag on a fineness-ratio-3 ogive at $M_\infty = 5.0$. In view of the good agreement between theory and the experimental results for the total drag coefficient at $\alpha = 0$ (fig. 5(b)), it is indicated that the assumptions employed regarding the type of boundary-layer flow are adequate for the present case. The lift and pitching-moment coefficients are also in good agreement with experiment at the lower angles of attack. It is clear that

the shock-expansion method tends to overestimate these coefficients at the higher angles of attack. This result is similar to that found for bodies of revolution (see, e.g., refs. 2 and 8) and, therefore, is not surprising. It should be noted from the results presented in references 2 and 8, however, that the accuracy of the method improves with increasing Mach number.

Ames Aeronautical Laboratory
National Advisory Committee for Aeronautics
Moffett Field, Calif., Sept. 16, 1958

REFERENCES

1. Eggers, A. J., Jr., Syvertson, Clarence A., and Kraus, Samuel: A Study of Inviscid Flow About Airfoils at High Supersonic Speeds. NACA Rep. 1123, 1953. (Supersedes NACA TN's 2646 and 2729)

2. Eggers, A. J., Jr., and Savin, Raymond C.: A Unified Two-Dimensional Approach to the Calculation of Three-Dimensional Hypersonic Flows, With Application to Bodies of Revolution. NACA Rep. 1249, 1955. (Supersedes NACA TN 2811)

3. Eggers, A. J., Jr., and Nothwang, George J.: The Ames 10- by 14-Inch Supersonic Wind Tunnel. NACA TN 3095, 1954.

4. Savin, Raymond C.: Application of the Generalized Shock-Expansion Method to Inclined Bodies of Revolution Traveling at High Supersonic Airspeeds. NACA TN 3349, 1955.

5. Beskin, L.: Determination of Upwash Around a Body of Revolution at Supersonic Velocities. Johns Hopkins Univ., Applied Physics Lab., CM 251, May 1946.

6. Rubesin, M. W., and Johnson, H. A.: A critical Review of Skin-Friction and Heat Transfer Solutions of the Laminar Boundary Layer of a Flat Plate. Trans. A.S.M.E., vol. 71, no. 4, May 1949, pp. 383-388.

7. Sommer, Simon C., and Short, Barbara J.: Free-Flight Measurements of Turbulent-Boundary-Layer Skin Friction in the Presence of Severe Aerodynamic Heating at Mach Numbers From 2.8 to 7.0. NACA TN 3391, 1955.

8. Syvertson, Clarence A., and Dennis, David H.: A Second-Order Shock-Expansion Method Applicable to Bodies of Revolution Near Zero Lift. NACA Rep. 1328, 1957. (Supersedes NACA TN 3527)

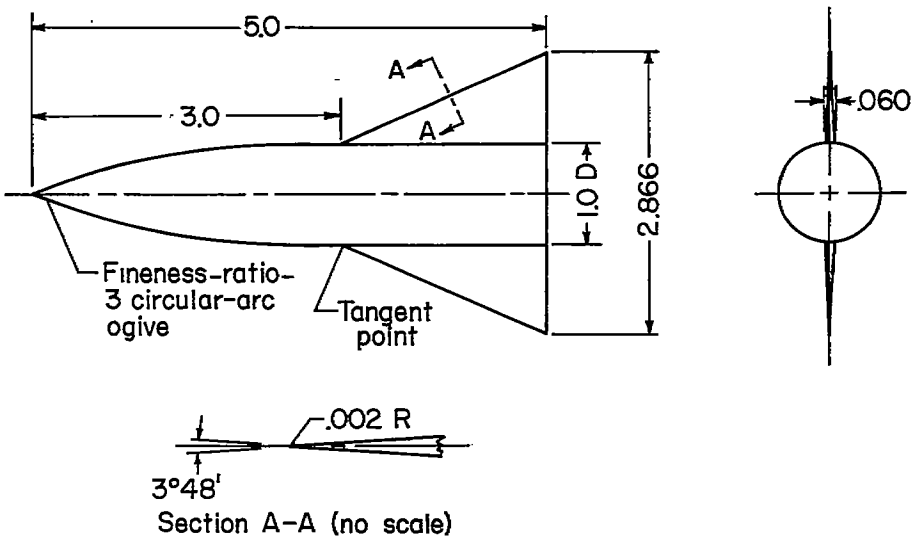

Section A-A (no scale)

Triangular-wing model

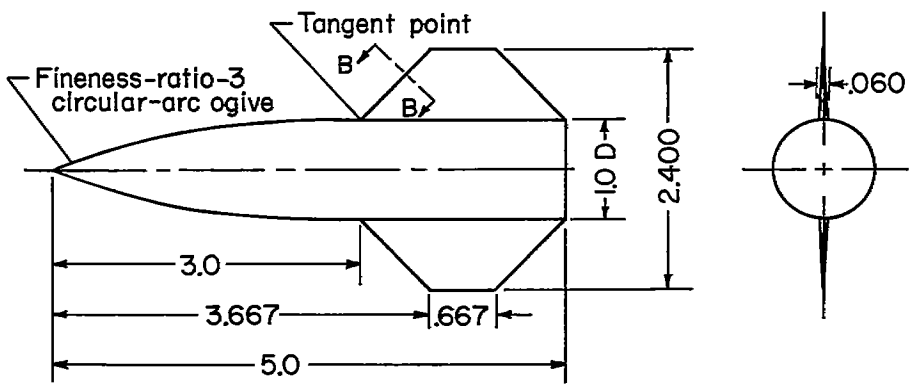

Section B-B (no scale)

All dimensions in inches
Plan form areas of both models are equal

Trapezoidal-wing model

Figure 1.- Details of test models.

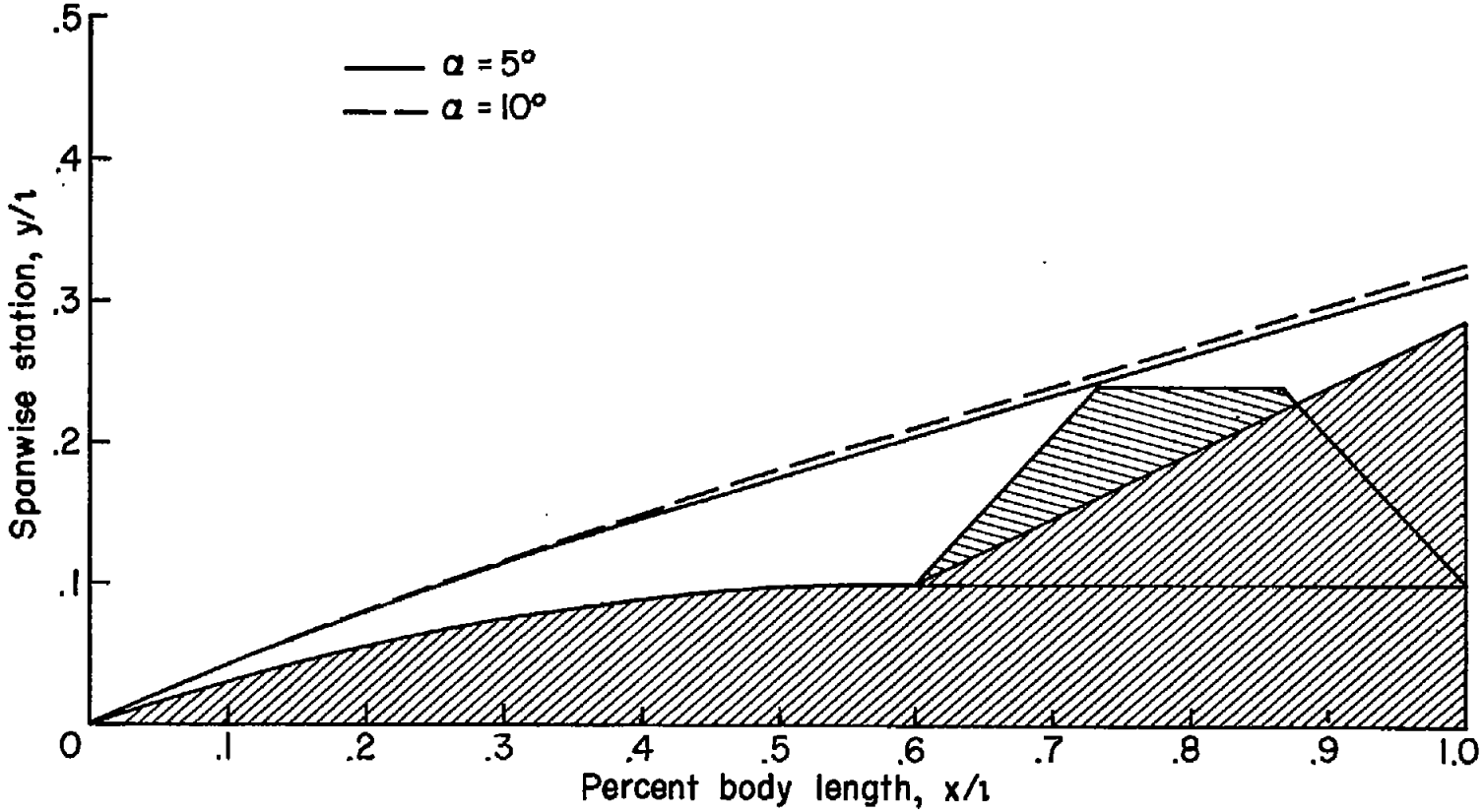

Figure 2.- Calculated shock-wave shapes at angles of attack of 5° and 10°; $M_\infty = 5.0$.

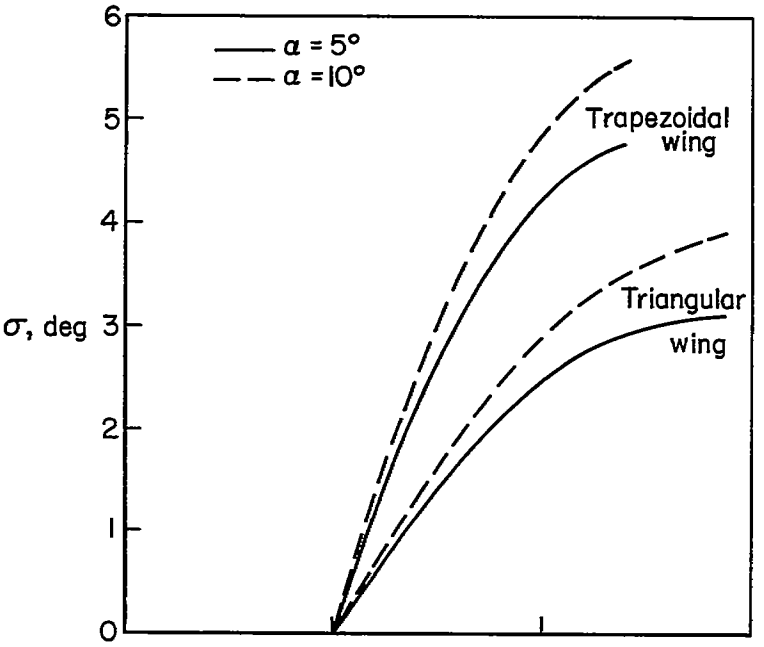

(a) Variation of sidewash angle.

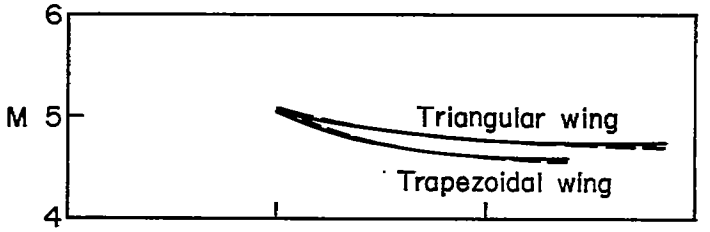

(b) Variation of Mach number.

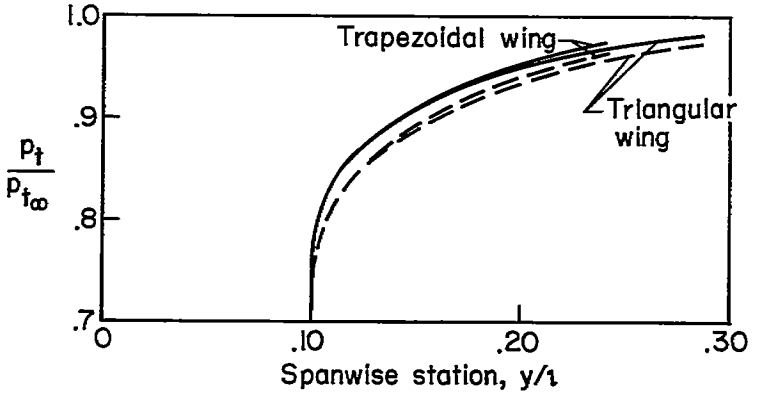

(c) Variation of total pressure.

Figure 3.- Calculated flow conditions at the wing leading edges.

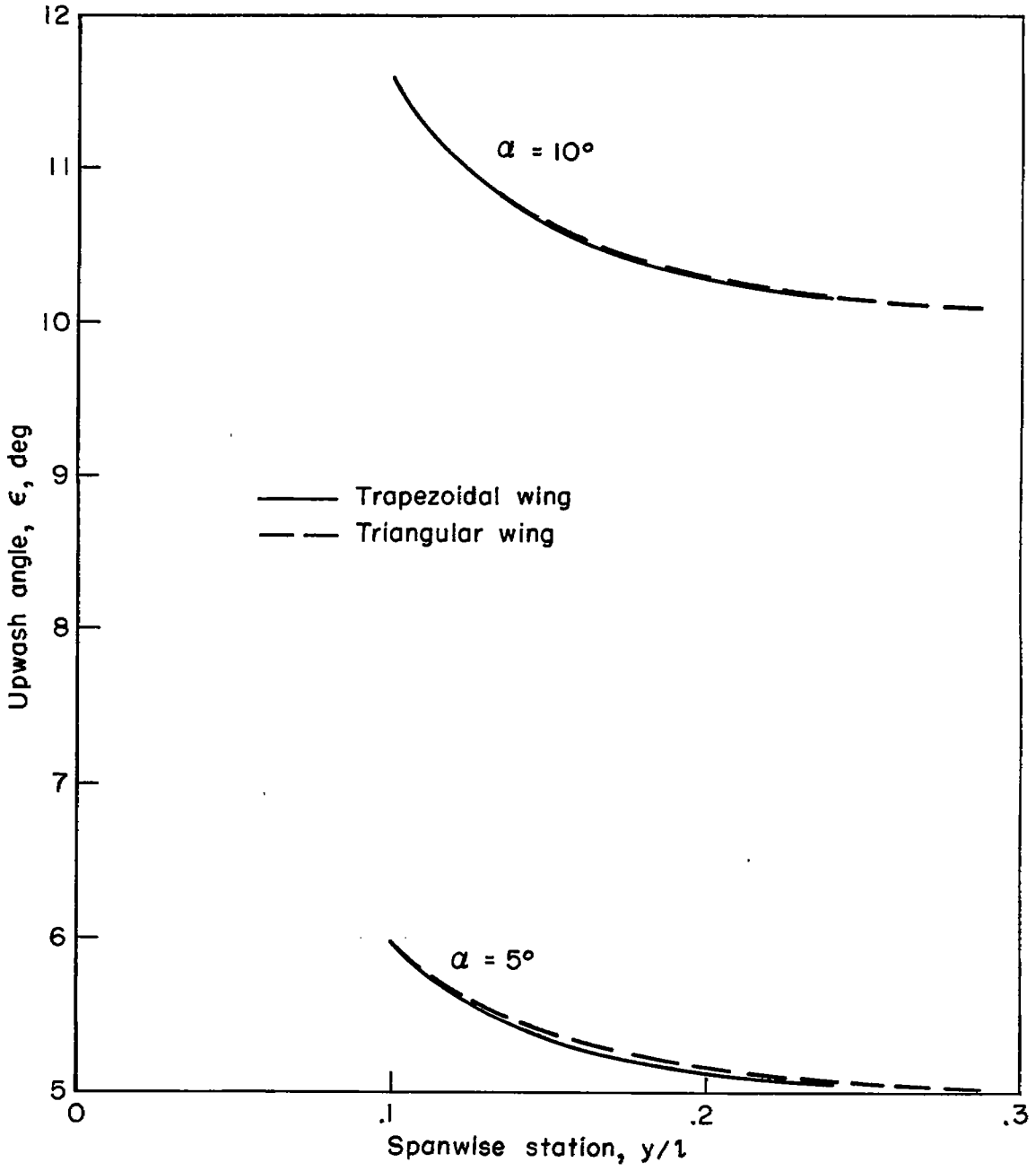

Figure 4.- Variation of upwash angle along the leading edges of the wings.

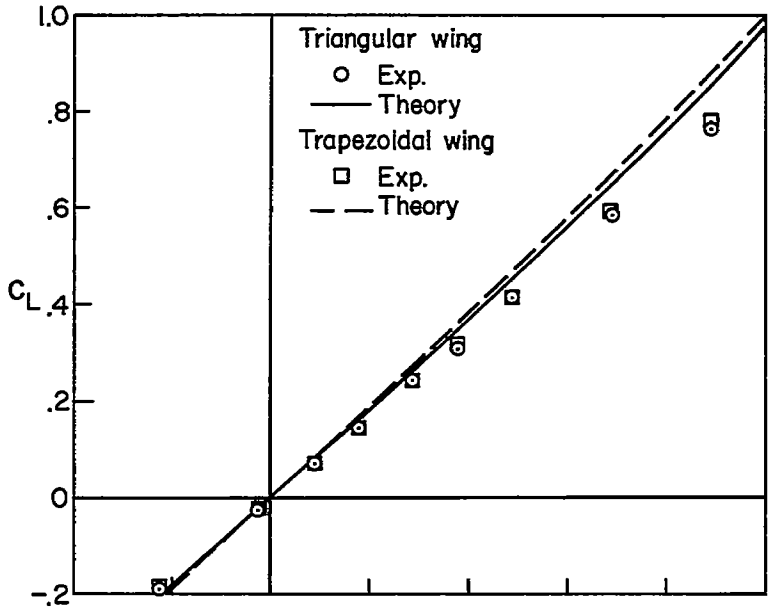

(a) Lift coefficient.

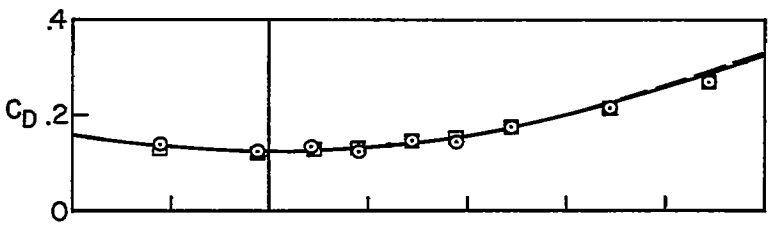

(b) Drag coefficient.

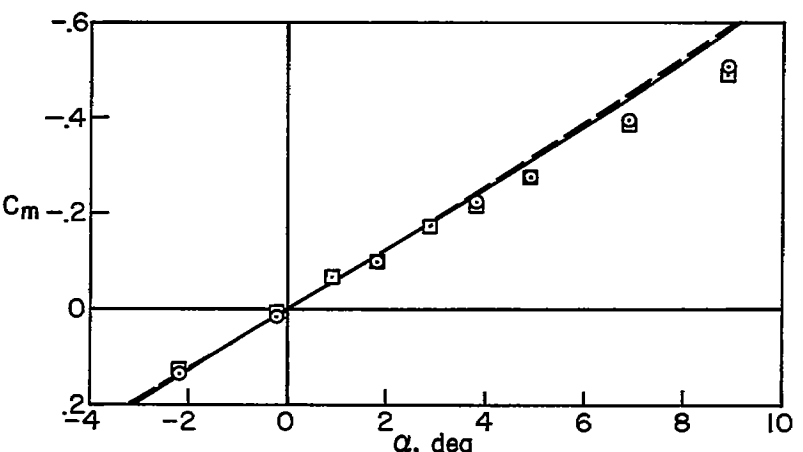

(c) Pitching-moment coefficient.

Figure 5.- Comparison of theoretical and experimental force and moment characteristics at $M_\infty = 5.0$.